CHAPTER 177

Wave Diffractions by Rows of Vertical Cylinders of Arbitrary Cross Section

Akinori Yoshida*, Norio Iida**, and Keisuke Murakami***

1. Introduction

Wave diffractions by a number of (a group of or a row of) vertical cylinders have been investigated in connection with, e.g., multilegged offshore structures (Spring and Monkmeyer(1974), Ohkusu(1974), Chakrabarti(1978), Mciver and Evans(1984), etc.); Wave-Power absorption devices (Miles (1983), Falnes(1984), Kyllingstad(1984), etc.); Wave barrier systems (Massel(1976), Kakuno and Oda(1986), etc.). Most of the previous works were, however, mainly aimed at the wave diffractions by cylinders of circular cross section and/or by cylinders of relatively small dimensions compared to wave length.

In this paper, we describe a simple yet versatile analytical method to solve wave diffractions by infinite rows of vertical cylinders. In the method, it is assumed, in addition to usual linearised small amplitude assumptions, that: the row of cylinders is composed of infinite number of surface-piercing evenly spaced equal cylinders fixed on sea bottom; incident wave direction is perpendicular to the row; the number of rows may be arbitrary, at least in principle; the cross sectional shape of the cylinders may be arbitrary as long as it is symmetrical with respect to the incident wave ray; and the cylinders are relatively large compared to incident wave length so that inertial forces are predominant to drag forces.

2. Formulation

We consider the diffractions of a regular plane wave by a row or rows of surface-piercing vertical cylinders fixed in water of uniform depth h. It is assumed that the row is composed of infinite number of equal cylinders evenly spaced (2b distance between adjacent cylinders) and that a plane

* Associate prof., Dept. of Civil Engineering Hydraulics, Kyushu University, 812 Fukuoka, Japan
** Engineer, Japan Port Consultant Ltd., Japan
*** Graduate Student, Kyushu University, 812 Fukuoka, Japan

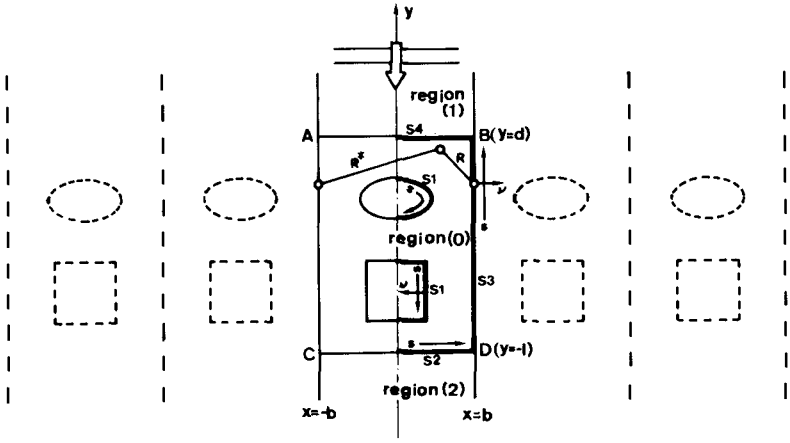

Figure 1. Definition sketch

wave of small amplitude ζ_0, radian frequency σ, wave number k, is incident on the row at right angle. Thus, the wave motion is periodic along the row of cylinders. This situation is equivalent to wave diffraction for a cylinder placed midway in a wave tank of the same width as the spacing interval 2b (e.g., See Sorokosz (1980), Taylor and Hung(1986)).

In the following formulation, we solve the equivalent problem by using an integral-equation and Fourier expansion techniques similar to that adopted by Sorokosz(1980): here in the present method, however, complicated mathematical form of Green function is not needed.

Cartesian co-ordinates are taken with the x and y axes in the horizontal plane of the water surface and the z axis directed vertically upwards. The row is arranged along x axis. A sketch of the horizontal section is given in figure 1.

The fluid is assumed to be inviscid and incompressible and the fluid motion irrotational so that it can be described by a velocity potential which may be expressed in the form

$$\Phi(x, y, z, t) = (g\zeta_0/\sigma)\phi(x, y)Z(z)\exp(i\sigma t) \qquad \ldots\ldots\ldots\ldots(1)$$

in which g is acceleration of gravity; $\phi(x,y)$ is dimensionless function which represents horizontal distribution of the velocity potential; $Z(z)=\cosh(k(z+h))/\cosh(kh)$; i = imaginary quantity ($\sqrt{-1}$).

Since the velocity potential satisfies Laplace equation, $\phi(x,y)$ satisfies the following Helmholtz equation,

$$\nabla^2\phi(x, y)+k^2\phi(x, y)=0 \qquad \cdots\cdots\cdots\cdots(2)$$

Now, introducing imaginary boundaries AB (indicated by S4 at y=d) and CD (indicated by S2 at y=-1) as shown in figure 1, we divide the fluid region into three regions, upstream region (1), downstream region (2) and truncated inner region (0).

The inner region (0) is a closed fluid region enclosed with the imaginary boundaries S2 and S4, the cylinder (indicated by S1) and the walls of the wave tank (indicated by S3). Thus, applying Green's theorem to the dimensionless function $\phi_0(x,y)$ in the inner region (0) which satisfies Helmholtz equation (2), it can be expressed by the following Green's Identity Formula:

$$\phi_0(X)=-\frac{i}{\alpha}\int_{S1+S2+S3+S4}\left\{\phi_0(X_b)\frac{\partial}{\partial\nu}G(kR)-G(kR)\frac{\partial}{\partial\nu}\phi_0(X_b)\right\}ds \qquad \cdots(3)$$

where $G(kR)=H_0^{(1)}(kR)+H_0^{(1)}(kR^*)$;

$H_0^{(1)}$ is the Hankel function of the first kind and of order 0; X denotes the co-ordinates (x,y) of any point in the inner region (0) and X_b on the boundary; $R=|X-X_b|$ and $R^*=|X-X_b^*|$ (X_b^* denotes the reflected image point of X_b with respect to the center line of the wave tank.); ν is the outward normal to the boundary; $\alpha=2$ when X is on the boundary and othewise $\alpha=4$.

The integration is taken counterclockwise and along a half of the boundary (indicated by thick lines in figure 1) because the fluid motion is symmetric with respect to the center line of the wave tank.

By representing the dimensionress function of the reflected wave potential and the transmitted wave potential with φ_1 and φ_2, respectively, the function ϕ_1 in the upstream region and ϕ_2 in the downstream region may be written as

$$\phi_1(x,y)=\exp(iky)+\varphi_1(x,y) \qquad \cdots\cdots\cdots\cdots(4)$$

$$\phi_2(x,y)=\varphi_2(x,y) \qquad \cdots\cdots\cdots\cdots(5)$$

The function φ_1 and φ_2 also satisfy Helmholtz equation

$$\nabla^2\varphi(x, y)+k^2\varphi(x, y)=0 \qquad \cdots\cdots\cdots\cdots(6)$$

Applying the method of the separation of variables ($\varphi(x,y)=X(x)Y(y)$) to (6), we obtain the following ordinary differential equations,

$$\left.\begin{aligned} &d^2X/dx^2+k_x^2X=0 \\ &d^2Y/dy^2+k_y^2Y=0 \\ &k_x^2+k_y^2=k^2 \end{aligned}\right\} \qquad \cdots\cdots\cdots\cdots\cdots\cdots(7)$$

Solving (7) under now-flow condition on the wave tank wall and under condition that $\varphi_1(x,y)$ represents waves propagating toward the upstream direction and $\varphi_2(x,y)$ waves propagating toward the downstream direction, we obtain

$$\varphi_1(x,y)=\sum_{n=0}^{\infty} C_n\beta_n(y)\cos(n\pi x/b) \qquad \cdots\cdots\cdots\cdots\cdots\cdots(8)$$

$$\varphi_2(x,y)=\sum_{n=0}^{\infty} D_n\bar{\beta}_n(y)\cos(n\pi x/b) \qquad \cdots\cdots\cdots\cdots\cdots\cdots(9)$$

where

$$\left.\begin{aligned} \beta_n(y)&=\exp\{-iy\sqrt{k^2-(n\pi/b)^2}\} \\ \bar{\beta}_n(y)&=\exp\{iy\sqrt{k^2-(n\pi/b)^2}\} \end{aligned}\right\} \qquad \cdots\cdots\cdots\cdots\cdots(10)$$

For n which satisfies kb>n (n=0,1,...), $\beta_n(y)$ and $\bar{\beta}_n(y)$ represent progressive wave modes, and otherwise (except for n when kb=n) exponentially decreasing stationary wave modes. For the case of kb=n, (8) and (9) give no-propagating wave mode and imply a standing wave exists across the wave tank.

Equations (8) and (9) show the Fourier series expansion of the dimensionless functions φ_1 and φ_2 across the wave tank, thus for example on the imaginary boundary S4 (at y=d), the coefficients $C_n\beta_n(d)$ can be written as

$$C_n\beta_n(d)=\frac{2e}{b}\int_0^b \varphi_1(x,d)\cos\frac{n\pi x}{b}\,dx \qquad \cdots\cdots\cdots\cdots\cdots(11)$$

where e=1/2 (n=0) and e=1 (n≠0).
Consequently, we obtain the expression of the dimensionless function $\phi_1(x,y)$ in the upstream region (1) as

$$\phi_1(x,y)=\exp(iky)+\sum_{n=0}^{\infty}\frac{\beta_n(y)}{\beta_n(d)}\left\{\frac{2e}{b}\int_0^b \varphi_1(s,d)\cdot\cos\frac{n\pi s}{b}\,ds\right\}\cos\frac{n\pi x}{b} \quad \cdots(12)$$

In the same way, in the downstream region (2), we obtain

$$\phi_2(x,y)=\sum_{n=0}^{\infty}\frac{\bar{\beta}_n(y)}{\bar{\beta}_n(-l)}\left\{\frac{2e}{b}\int_0^b \varphi_2(s,-l)\cdot\cos\frac{n\pi s}{b}\,ds\right\}\cos\frac{n\pi x}{b} \quad \cdots(13)$$

The boundary conditions for the inner region (0) can be written

$$\partial\phi_0/\partial\nu=0 \qquad (S1 \qquad S3) \qquad \ldots\ldots\ldots\ldots\ldots\ldots(14)$$

$$\left.\begin{aligned}\phi_0&=\phi_2\\ \partial\phi_0/\partial\nu&=\partial\phi_2/\partial\nu\end{aligned}\right\}\ (S2:\ y=-l) \qquad \ldots\ldots\ldots\ldots\ldots(15)$$

$$\left.\begin{aligned}\phi_0&=\phi_1\\ \partial\phi_0/\partial\nu&=\partial\phi_1/\partial\nu\end{aligned}\right\}\ (S4:\ y=d) \qquad \ldots\ldots\ldots\ldots\ldots(16)$$

By applying (4),(5),(12) and (13) to (15) and (16), equations (15) and (16) are rewritten as

$$\left.\begin{aligned}&\phi_0(x,-l)=\varphi_2(x,-l)\\ &\left.\frac{\partial\phi_0}{\partial\nu}\right|_{y=-l}=\sum_{n=0}^{\infty}\frac{2e}{b}\alpha_n\left\{\int_0^b\varphi_2(s,-l)\cdot\cos\frac{n\pi s}{b}ds\right\}\cdot\cos\frac{n\pi x}{b}\\ &\phi_0(x,d)=\exp(ikd)+\varphi_1(x,d)\\ &\left.\frac{\partial\phi_0}{\partial\nu}\right|_{y=d}=ik\exp(ikd)+\sum_{n=0}^{\infty}\frac{2e}{b}\alpha_n\left\{\int_0^b\varphi_1(s,d)\cdot\cos\frac{n\pi s}{b}ds\right\}\cdot\cos\frac{n\pi x}{b}\end{aligned}\right\}\ldots(17)$$

where $\alpha_n=\sqrt{k^2-(n\pi/b)^2}$

In order to solve the integral equation (3) under these boundary conditions, we divide the boundary, S1, S2, S3 and S4, into a number of small elements ΔS_j (j=1-N1, 1-N2, 1-N3, 1-N4 on S1, S2, S3 and S4, respectively). Now, assuming that ϕ_0 and its normal derivative $\partial\phi_0/\partial\nu$ are uniform on each element, and denoting them by $\phi_0(j)$ and $\bar{\phi}_0(j)$, we can approximate (3) by the following discretaised equation,

$$\phi_0(X)=\left\{\sum_{j=1}^{N1}+\sum_{j=1}^{N2}+\sum_{j=1}^{N3}+\sum_{j=1}^{N4}\right\}(\bar{G}_{Xj}\phi_0(j)-G_{Xj}(j)\,\bar{\phi}_0(j)) \qquad \ldots\ldots(18)$$

where

$$\left.\begin{aligned}G_{Xj}&=-\frac{i}{\alpha}\int_{\Delta S_j}\{H_0^{(1)}(kR)+H_0^{(1)}(kR^*)\}\,ds\\ \bar{G}_{Xj}&=-\frac{i}{\alpha}\int_{\Delta S_j}\frac{\partial}{\partial\nu}\{H_0^{(1)}(kR)+H_0^{(1)}(kR^*)\}\,ds\end{aligned}\right\} \qquad \ldots\ldots(19)$$

When the point X is on the center of any element ΔS_j, equation (18) gives a finite set of linear relations between $\phi_0(j)$ and $\bar{\phi}_0(j)$ as

$$\phi_0(i)=\left\{\sum_{j=1}^{N1}+\sum_{j=1}^{N2}+\sum_{j=1}^{N3}+\sum_{j=1}^{N4}\right\}(\bar{G}_{ij}\phi_0(j)-G_{ij}\bar{\phi}_0(j)) \quad \ldots\ldots\ldots\ldots\ldots(20)$$

$$(i=1\sim N1,\ 1\sim N2,\ 1\sim N3,\ 1\sim N4)$$

Applying the boundary conditions (14) and (17) to (20), we obtain

$$\sum_{j=1}^{N1}(\bar{G}_{ij}-\delta_{ij})\phi_0(j)+\sum_{j=1}^{N2}\left\{(\bar{G}_{ij}-\delta_{ij})\ -\sum_{p=1}^{N2}G_{ip}Q_{jp}\right\}\varphi_2(j)$$

$$+\sum_{j=1}^{N3}(\bar{G}_{ij}-\delta_{ij})\phi_0(j)\ +\sum_{j=1}^{N4}\left\{(\bar{G}_{ij}-\delta_{ij})-\sum_{p=1}^{N4}G_{ip}Q_{jp}\right\}\varphi_1(j)$$

$$=-\exp(ikd)\sum_{j=1}^{N4}\{(\bar{G}_{ij}-\delta_{ij})+ikG_{ij}\} \quad \ldots\ldots(21)$$

where $\delta_{ij}=1$ (i=j) and $\delta_{ij}=0$ (i≠j);

$$Q_{jp}=\sum_{n=0}^{\infty}\frac{2e}{b}\alpha_n\Delta S_p\cos\frac{n\pi x_j}{b}\cos\frac{n\pi x_p}{b} \quad \ldots\ldots\ldots\ldots(22)$$

Since equation (21) holds for every i-th element, it provides (N1+N2+N3+N4) linear equations with respect to the same number of unknown quantities, ϕ_0(j) on S1, φ_2(j) on S2, ϕ_0(j) on S3 and φ_1(j) on S4. Thus, solving these linear equations and using the boundary condition (17), we can obtain ϕ_0(j) and $\bar{\phi}_0$(j) for all of the boundary element. The function (X) at any point in the inner region (0) can be evaluated by (18), and ϕ_1(X) and ϕ_2(X) by discretaised form of (12) and (13), respectively.

The ratio of the wave amplitude ζ(X) at any point X to the incident wave amplitude ζ_0 is given by

$$|\zeta(X)/\zeta_0|=|\phi(X)| \quad \ldots\ldots\ldots\ldots\ldots\ldots(23)$$

The pressure p at the cylinder surface are evaluated from the relation $p=-\rho(\partial\Phi/\partial t)$. Thus, the wave force F acting on the cylinder can be obtained from the integration of p around the cylinder surface

$$F/2\rho g\zeta_0h^2[\tanh kh/kh]=\left|\sum_{j=1}^{N}\phi_0(j)\Delta x_j/h\right| \quad \ldots\ldots\ldots\ldots\ldots\ldots(24)$$

where ρ is the density of water; Δx_j is the x-compornent of ΔS_j on the cylinder; N is the number of the elements on the cylinder.

The reflection and transmission coefficients can be evaluated from energy flux of the reflected wave and the transmitted wave across the imaginary boundaries. The energy

flux of the reflected wave E_r may be written as

$$E_r=\frac{1}{bT}\int_0^b\int_0^T\int_{-h}^0\left\{\rho Re\left[\frac{\partial\Phi_r}{\partial t}\right]Re\left[\frac{\partial\Phi_r}{\partial y}\right]\right\}dz\,dt\,dx \qquad \text{.....(25)}$$

where Φ_r denotes the velocity potential of the reflected wave and it is given from (1), (4) and (8) by

$$\Phi_r=\frac{g\zeta_0}{\sigma}\left\{\sum_{n=0}^{\infty}C_n\beta_n(y)\cos\frac{n\pi x}{b}\right\}Z(z)\exp(i\sigma t) \qquad \text{.....(26)}$$

Substituting (26) into (25), we have

$$\frac{E_r}{E_i}=\sum_{n=0}^{n^*}\frac{\bar{\varepsilon}\alpha_n}{k}|C_n|^2 \qquad \text{.....(27)}$$

where E_r indicates the energy flux of the incident wave given by $(\rho g\zeta_0^2/8)(1+2kh/\sinh 2kh)(\sigma/k)$; $\bar{\varepsilon}=1$ (n=0) and $\bar{\varepsilon}=1/2$ ($n\neq 0$); n is the largest integer value among n's satisfying kb>n. Thus the reflection coefficient K_r is given by

$$K_r=\sqrt{\sum_{n=0}^{n^*}\frac{\bar{\varepsilon}\alpha_n}{k}|C_n|^2} \qquad \text{.....(28)}$$

In the same way, from the energy flux of the transmitted wave across the imaginary boundary CD, the transmission coefficient K_t is given by

$$K_t=\sqrt{\frac{E_t}{E_i}}=\sqrt{\sum_{n=0}^{n^*}\frac{\bar{\varepsilon}\alpha_n}{k}|D_n|^2} \qquad \text{.....(29)}$$

and the following relations should be satisfied

$$\sum_{n=0}^{n^*}\frac{\bar{\varepsilon}\alpha_n}{k}\{|C_n|^2+|D_n|^2\}=1 \qquad \text{.....(30)}$$

3. Numerical Calculations and Experimental Verifications

For the numerical analysis, the infinite series of (17) and (22) are replaced by a finite sum upto N^*. The integrations in (17) are evaluated with the following discrete form

$$\int_0^b\varphi(s,d)\cos\frac{n\pi s}{b}ds\approx\sum_{p=1}^{N_4}\varphi(p)\cos\frac{n\pi\xi_p}{b}\Delta S_p \qquad \text{.....(31)}$$

and this shows discrete Fourie Transform of φ, thus, it is clear, from the theorem of Finite Fourier Series approximation, that N^* should be the same number as that of thek^*

divided elements on the imaginary boundary.

Because the set of the imaginary boundaries is only for the creation of the enclosed fluid region to which Green's theorem is applied, the location of the imaginary boundaries has no physical grounds. Thus, the distance of the imaginary boundaries from the cylinder may be arbitrary and no significant difference occurs in numerical results. In the following numerical calculations, the locations of the imaginary boundaries were taken 3h away from the side of the cylinder and the size of the boundary elements were taken about $\Delta s_j/h=0.2$,

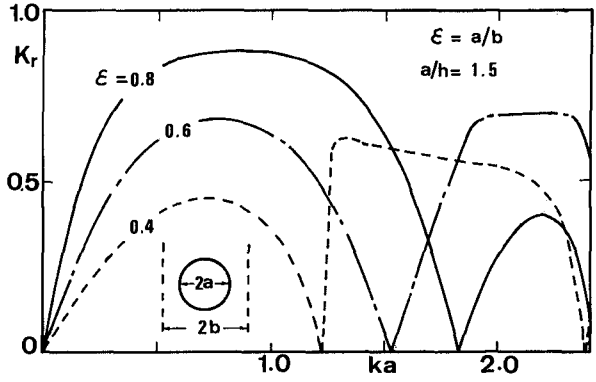

Figure 2. Reflection coefficient for a row of circular cylinders

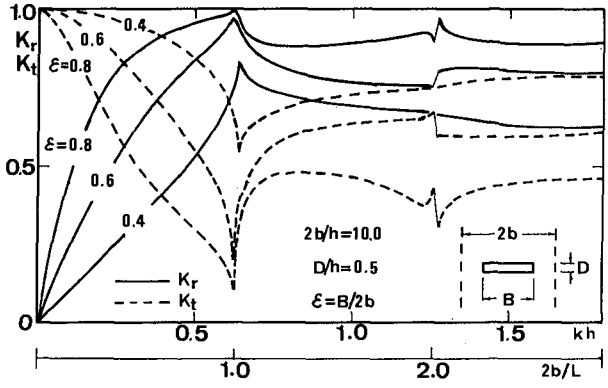

Figure 3. Reflection and transmission coefficients for a row of rectangular cylinders

Figure 2 shows the reflection coefficient for a single row of circular cylinders. The diameter of the cylinder 2a is fixed to 2a/h=3.0 and three different spacing between the cylinders are made to give ε(=2a/2b) of 0.4, 0.6 and 0.8. The reflection characteristics are very much dependent on the incident wave number. Near singular wave number (kb=n) K_r decreases to zero, namely, waves transmits through the cylinder barrier with almost no wave reflection. It is noted that the smaller spacing between the cylinders does not necessarily mean the larger wave reflection.

Figure 3 shows the reflection and transmission coefficients for a single row of rectangular cylinders. The spacing 2b is fixed to 2b/h=10.0, and the width B of the cylinder is changed to give ε(=B/2b) of 0.4, 0.6 and 0.8. The reflection characteristics much differ from those of the circular cylinders, and this shows that the cross-sectional shape of the cylinder is one of main factor for wave reflection-transmission characteristics. At the singular wave numbers where 2b/L=1.0, 2.0,...(L is the incident wave length), it is possible for a standing wave to exist across the wave tank (that is, along the row of the cylinders).

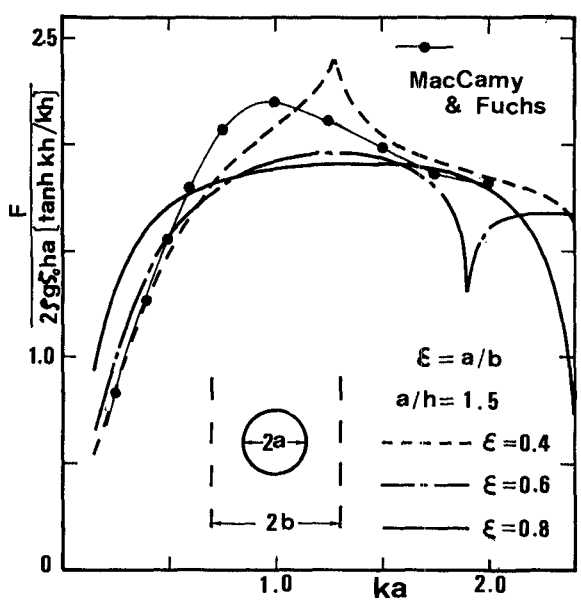

Figure 4. Wave forces for a row of circular cylinders

Wave forces corresponding to figures 2 and 3 are given in figures 4 and 5, respectively. Naturally the forces acting on the cylinders are in line with the direction of the incident wave. Thin solid curve with closed circle in figure 4 represents wave forces acting on a single cylinder in an open-sea given by MacCamy and Fuchs.

Figure 6 shows numerically calculated free surface amplitude around a square cylinder placed on the center line of the wave tank (the case of a row of square cylinders). It is noted that satnding waves appear in the x direction as well as in the upstream direction.

To verify the present method, we conducted wave tank experiments for a row of circular cylinders, a row of rectangular cylinders and two rows of circular cylinders. The wave tank (4m wide × 20m long × 0.6m deep) in the laboratory of Civil Engineering Hydraulics, Kyushu University was used. The diameter of the model cylinders

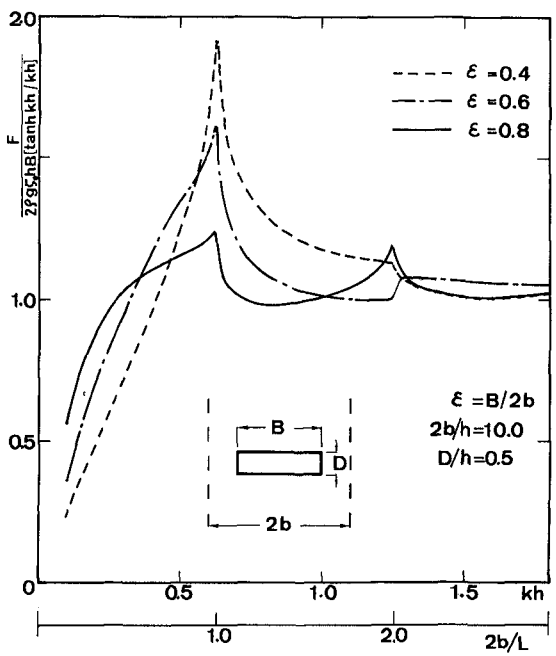

Figure 5. Wave forces for a row of rectangular cylinders

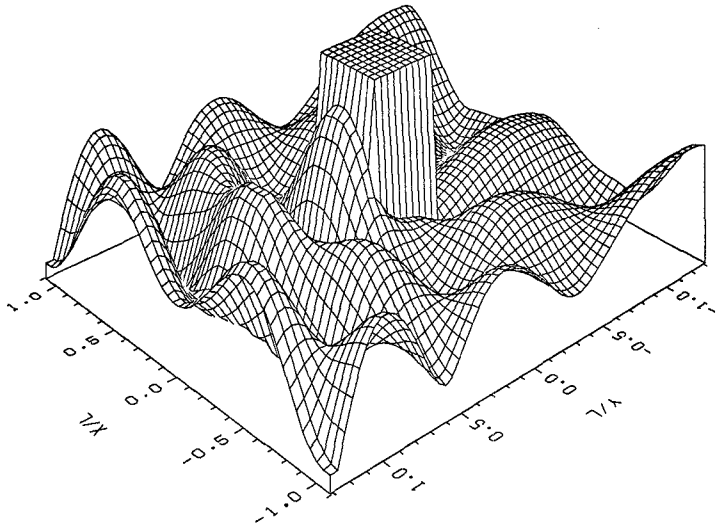

Figure 6. Perspective view of free surface amplitude for a row of square cylinders (kh=1.4, b/h=5.0, B/h=2.0; B is the side length of the square)

were 1.2m, and the size of the rectangular model was 2m by 0.2m. The water depth was kept 0.4m throughout the experiments.

Setting the model cylinders midway of the wave tank, we measured water surface elevation around the cylinders at 20cm by 20cm grid points with 6 capacity type wave gages. The total number of measured grid points were about 200.

The comparisons for perspective view of free surface amplitude between the theory and the experiments are shown in figures 7, 8 and 9. Although the free surface amplitudes drawn from experimental data show rather rough surface compared to the theoretically obtained ones, especially when the free surface is seriously disturbed (for example, figure 9.) because of measured grid points are coarse, overall agreements between the theory and experiments for free surface amplitude are very good.

More precise comparison is given in figure 10 with respect to a contour map of water surface elevation. The number in the contour lines indicates the ratio of free surface amplitude to the incident wave amplitude. Again, very good agreement between the theory and experiment is confirmed.

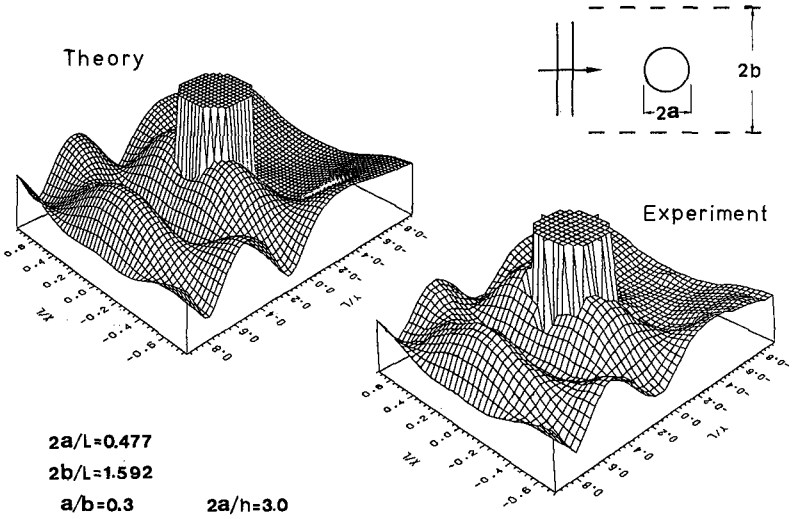

Figure 7. Comparison between theory and experiment for a row of circular cylinders

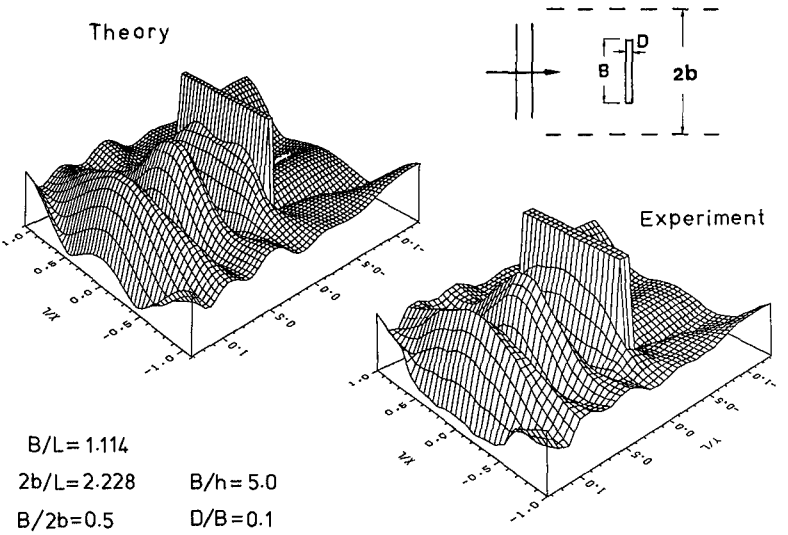

Figure 8. Comparison between theory and experiment for a row of rectangular cylinders

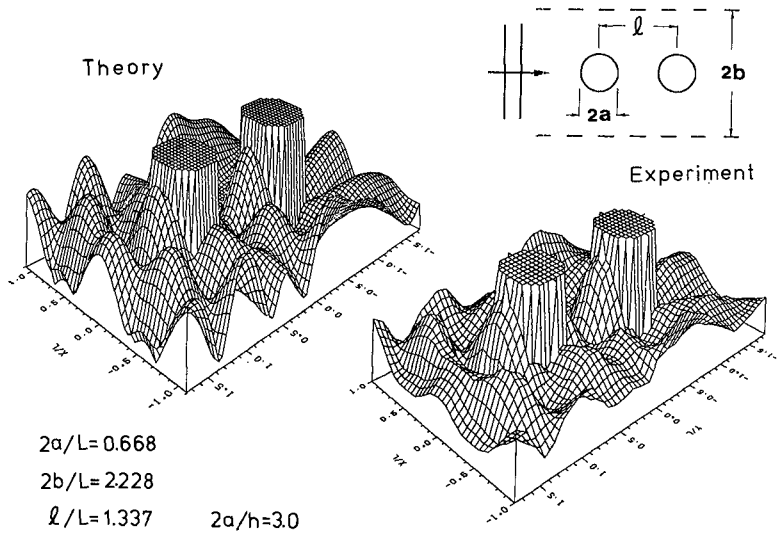

Figure 9. Comparison between theory and experiment for two rows of circular cylinders

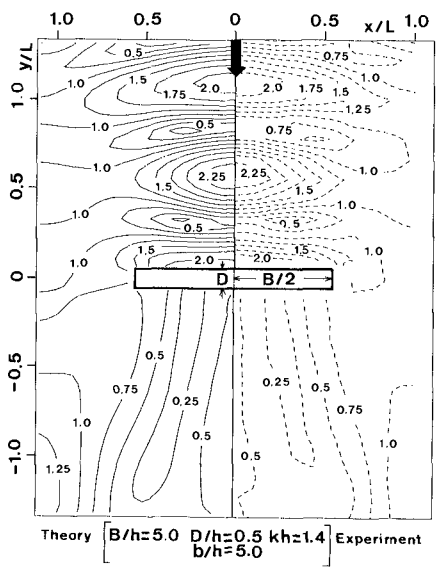

Figure 10. Contour map of free surface amplitude corresponding to figure 8.

4. Conclusions

A simple analytical method using an integral-equation technique has been described for solving wave diffractions by rows of surface-piercing vertical cylinders evenly spaced on sea bottom. The feature of the present method is its easiness to treat diffraction problems of rows of cylinders of arbitrary cross-section and plural row of cylinders: changing the co-ordinates of the boundary elements along the cylinder is the only requirement for variations in the number of the rows and the cross sectional shape of the cylinders.

The method can be easily extended to the case for floating cylinders with flat bottom and for submerged cylinders with flat top, by further applying the Green's Identity Formula for the expression ofthe wave motion in the region between the sea bottom and the bottom of the cylinder and in the region between the free surface and the top of the submerged cylinder. Such cases are related to the problems that frequently occur in Coastal Engineering field, e.g., reflection and transmission problems for rows of floating breakwaters, rows of submerged breakwaters, etc.

The present method is limited to the case that an incident wave direction is perpendicular to the rows of cylinders. More realistic case of oblique incidence needs further study though several studies have been made for a row of circular cylinders by, e.g., Massel (1976) and Miles (1983).

REFERENCES

1 CHAKRABARTI, S.K. (1978). Wave forces on multiple vertical cylinders. Proceedings of American Society of Civil Engineers, 104(ww2): 147-161

2 FALNES, J. (1984). Wave-power absorption by an array of attenuators oscillating with unconstrained amplitudes. Applied ocean research, 6(1): 16-22

3 KYLLINGSTAD,K. (1984). A low-scattering approximation for the hydrodynamic interactions of small wave-power devices, Applied Ocean Research, vol.6, No.3:132-139

4 KAKUNO, S. and ODA, K. (1986). Boundary value analysis on the interaction of cylinder arrays of arbitrary cross-section with a train of uniform waves, Proceedings of Japanese Society of Civil Engineers, No.369, (in japanese)

5 MASSEL, R.M. (1976). Interaction of water waves with cylinder barrier. Proceedings of American Society of Civil Engineers, 102(ww2): 165-187

6 MILES, J.W. (1983). Surface-wave diffraction by a periodic row of submerged ducts. Journal of fluid mechanics, 128: 155-180

7 McIVER, P. and EVANS, D.V. (1984). Approximation of wave forces on cylinder arrays. Applied ocean research, 6(2): 101-107
8 OHKUSU, M. (1974). Hydrodynamic forces on multiple cylinders in waves, Proc. Int. Sympo. Dynamics of Marine Vehicles and Structures in Waves
9 SPRING, B.H. and MONKMEYER, P.L. (1974). Interaction of plane waves with vertical cylinders. Proceedings of the fourteenth coastal engineering conference, 3: 1828-1847
10 SOROKOSZ, M.A. (1980). Some relations for bodies in a canal, with an application to wave-power absorption. Journal of fluid mechanics, 99(1): 145-162
11 TAYLOR, R.E. and HUNG, S.M. (1985). Mean drift forces on an articulated column oscillating in a wave tank. Applied ocean research, 7(2): 67-78